Proceedings of The Thirteenth (2003) International Offshore and Polar Engineering Conference
Honolulu, Hawaii, USA, May 25−30, 2003

ISBN 1−880653-60−5 (Set); ISSN 1098−6189 (Set)

Modeling of Breaking and Post-breaking Waves on Slopes by Coupling of BEM and VOF Methods

Christophe Lachaume[1], *Benjamin Biausser*[1], *Stéphan T. Grilli*[2], *Phillippe Fraunié*[1], *and Stéphan Guignard*[3]
1. LSEET, Univ. de Toulon et du Var, La Garde, France
2. Ocean Engng. Dpt., Univ. of Rhode Island, Narragansett, RI, USA
3. ESIM, Marseille, France.

ABSTRACT

We study the shoaling, breaking, and post-breaking of waves, in two dimensions, using a model, i.e., a Numerical Wave Tank, based on coupling a Boundary Element Model, solving potential flow equations, to a Volume Of Fluid model, solving Navier-Stokes equations. We apply the model to calculating the transformation of solitary waves over plane slopes. We compare results to existing laboratory experiments. The agreement is quite good between computations and measurements. Finally, we compute properties of waves breaking over various slopes, such as shape, internal velocities and type of breaking.

KEYWORDS : Nonlinear nearshore wave transformations, wave shoaling and breaking, numerical wave tank, boundary element method, Volume Of Fluids method.

INTRODUCTION

As ocean waves approach the shore, they are affected by the decreasing depth, which causes gradual changes in wave celerity, height and shape. These changes are usually referred to as *wave shoaling*. Very close to shore, shoaling causes wave height to significantly increase and wavelength to decrease; hence, at some point, waves become too steep and break. One usually defines the breaking point (BP) as the location where waves have a vertical tangent on the front face; thus, beyond the BP, waves become unstable, overturn and break. The *surfzone* extends from the BP to shore, and this is a region of high vorticity, turbulence, and dissipation for the wave flow. Characteristics of waves at the BP largely define the way they break, and thus greatly influence surfzone dynamics, the design of structures used for coastal protection, and both the cross-shore and littoral sediment transports. For many beaches, cross-shore variations of bathymetry are predominent over longshore variations and, particularly close to shore, it is quite accurate, for all practical purposes, to study wave propagation in two dimensions (2D), in a vertical plane.

Comparisons of laboratory experiments with numerical models show that potential flow theory, with fully nonlinear free surface boundary conditions (FNPF), is very accurate for predicting the shape and kinematics of surface waves shoaling over a sloping bottom, up to the BP (e.g., Grilli *et al.*, 1994, 1997; Ohyama *et al.*, 1994; Grilli and Horrillo, 1999). Actually, FNPF theory seems to be quite accurate, even beyond the BP, up to the instant of impact of a breaker jet on the free surface (Li and Raichlen, 1998); further than this, however, the theory breaks down (e.g., Fig. 1, curve f).

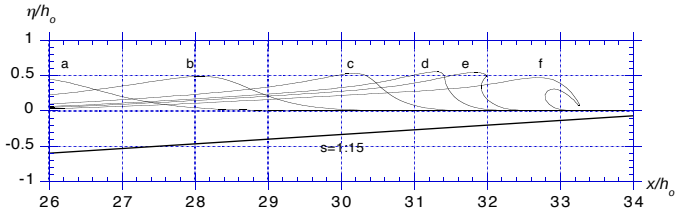

Fig. 1 : Shoaling and breaking of a solitary wave with $H_o/h_o = 0.45$, over a 1:15 slope in the FNPF-BEM model by Grilli *et al.* (1997).

FNPF equations are typically solved in a boundary integral formulation, based on free space Green's function or (in 2D) on Cauchy integral theorem, coupled to a higher-order mixed Eulerian-Lagrangian time updating of both the boundary geometry and potential. Many 2D-FNPF models and, more recently, a few three-dimensional FNPF models, have been proposed, based on these numerical methods. When implemented in the physical space (by contrast with conformally mapped or periodic space), FNPF models are often referred to in the literature as *Numerical Wave Tanks* (NWT), because they emulate the functionality

of laboratory tanks, i.e., wave generation, propagation and radiation/absorption (see below and review by Kim *et al.*, 1999).

NWTs based on a higher-order Boundary Element Method (BEM) have proved very efficient and accurate for calculating the propagation and shoaling of ocean waves, over arbitrary bottom topography, up to overturning of a wave (e.g., Grilli and Subramanya, 1996, Grilli *et al.*, 1994, 1997; Grilli and Horrillo, 1999). The limitation of BEM-NWTs to non-breaking waves has led to the development of various artificial methods for preventing breaking in computations. These methods are usually referred to as *absorbing beaches* (AB) (e.g., Grilli and Horrillo, 1997). Their principle is to absorb energy from incident waves, at the extremity of the NWT, before they start overturning, through a combination of surface pressure and lateral active absorption ("absorbing pistons"). Such ABs are thus essentially non-physical numerical tools, in the sense that, while globally absorbing wave energy, they do not dissipate it the way it occurs in nature, i.e., through the combined action of vorticity, turbulence, and viscosity within the fluid volume. Hence, results for wave shape and kinematics are quite approximate within the AB.

For many applications in coastal engineering, however, it is desirable to more accurately model the flow within breaking waves and thus solve the full Navier-Stokes (NS) equations. In surfzone hydrodynamics, the traditional approach has been to average NS equations over one wave period and to model turbulence and dissipation terms with semi-empirical formulae. To calculate details of the breaking wave flow in the time domain, however, NS equations must be solved on a sufficiently fine grid, resolving small scale turbulent features, and accounting for two fluids, air and water, and the possibility of pockets of air to be trapped within the fluid domain and for pieces of water to detach from the main computational domain.

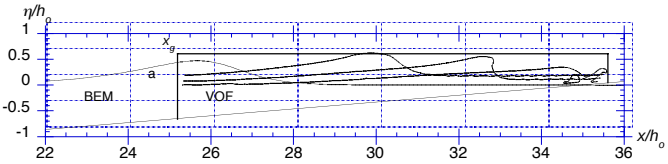

Fig. 2 : Principle of weak FNPF-BEM/NS-VOF model coupling. Shoaling of a solitary wave with incident height $H_o/h_o = 0.45$, over a 1:15 slope (curve a). Fluid velocities and pressures are calculated at a vertical gage at x_g and in VOF box. VOF model is initialized with wave a, and uses lateral BEM boundary conditions at x_g.

Improvements in computer power have recently made it possible to tackle such problems using models based on the Volume Of Fluid (VOF) method, which solve NS equations for free surface flow problems (Guignard et al., 2001). These models can solve equations on a grid covering the whole (air/water) fluid domain (unlike the BEM which only discretizes boundaries), and are able to accurately follow the motion of free surfaces and interfaces between fluids, represented by segments. VOF models also allow for air to be trapped within the fluid domain and for pieces of water to detach from the main computational domain. Hence, they are ideally suited for modeling breaking and post-breaking waves over a sloping bottom. VOF models, however, are computationally expensive and suffer from numerical diffusion, leading to artificial loss of wave energy (and elevation) over long distances of propagation.

In the present study, the key features and advantages of both BEM and VOF methods are exploited, by coupling these methods to perform two-dimensional wave shoaling and breaking computations (Fig. 2). The BEM method accurately and efficiently models wave shoaling over a sloping bottom, before breaking occurs. The VOF method calculates breaking and post-breaking waves at the top of the sloping bottom, on a refined local grid. Only solitary waves propagating over plane slopes are considered here.

Two types of coupling methodologies are implemented. In the first one, referred to as "weak coupling", the wave is propagated in the BEM domain, up to close to the breaking point, into a smaller region at the top of the slope, representing the VOF domain. Lateral (offshore) boundary conditions and internal velocity and pressure fields are then computed with the BEM, at the VOF grid cell centers, and computations are pursued in the VOF domain (Fig. 2). More details regarding this approach can be found in Guignard et al. (1999).

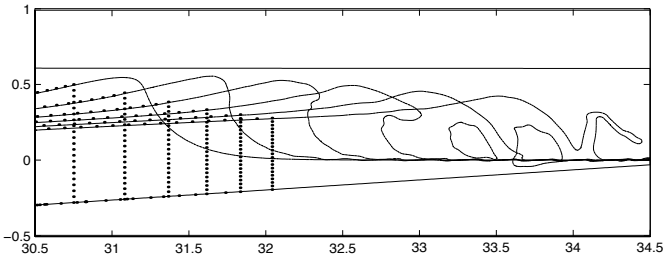

Fig. 3 : Principle of strong FNPF-BEM/NS-VOF model coupling. Same case as in Fig. 2. (——) VOF results; (•) BEM nodes.

In the second method, referred to as "strong coupling", a moving vertical matching boundary is used to specify/exchange boundary conditions in between both models, within a fluid region where both models overlap (Fig. 3).

Although both of these methods provide similar results for solitary waves, the second method makes it possible modeling periodic or irregular waves. This, however, will be left out for future work. In the present study, we apply the "weak coupling method" to the computation of properties, essentially shape and kinematics, of solitary waves breaking over plane slopes.

THE NUMERICAL WAVE TANK

BEM model

Grilli and Subramanya (1996) implemented an efficient and accurate two-dimensional (2D) BEM model solving fully nonlinear potential flow equations (FNPF; Fig. 1), i.e., continuity equation,

$$\nabla^2\phi = 0 \qquad \text{in } \Omega(t) \qquad (1)$$

for the potential, and the fully nonlinear kinematic and dynamic

free surface boundary conditions,

$$\frac{D\mathbf{r}}{Dt} = (\frac{\partial}{\partial t} + \mathbf{u}\cdot\nabla)\,\mathbf{r} = \mathbf{u} = \nabla\phi \qquad \text{on } \Gamma_f(t) \qquad (2)$$

$$\frac{D\phi}{Dt} = -gz + \frac{1}{2}\nabla\phi\cdot\nabla\phi - \frac{p_a}{\rho} \qquad \text{on } \Gamma_f(t) \qquad (3)$$

respectively, with $\mathbf{r}$, the position vector on the free surface, g the gravitational acceleration, z the vertical coordinate, p_a the pressure at the free surface, and ρ the fluid density; and a no-flow condition on the bottom,

$$\frac{\partial\phi}{\partial n} = 0 \qquad \text{on } \Gamma_b \qquad (4)$$

Boundary conditions on lateral boundaries Γ_{r1} and Γ_{r2} are discussed next.

Eq. (1) is transformed into a Boundary Integral Equation (BIE), using Green's 2nd identity, and solved by a Boundary Element Method (BEM). The BIE is expressed for N discretization nodes on the boundary, and M higher-order elements are defined to interpolate in between discretization nodes. In the present applications, quadratic isoparametric elements are used on lateral and bottom boundaries, and cubic elements ensuring continuity of the boundary slope are used on the free surface. In these elements, referred to as Mid Cubic Interpolation (MII) elements, both geometry and field variables are interpolated between each pair of nodes, using the mid-section of a four-node "sliding" isoparametric element. Detailed expressions of BEM integrals (regular, singular, quasi-singular) are given in Grilli and Subramanya (1996), for both isoparametric and MII elements.

Free surface boundary conditions (2) and (3) are time integrated based on two second-order Taylor series expansions expressed in terms of a time step Δt and of the Lagrangian time derivative, D/Dt, for ϕ and $\mathbf{r}$. First-order coefficients in the series correspond to free surface conditions (2) and (3), in which ϕ and $\partial\phi/\partial n$ are obtained from the BEM solution of the BIE for (ϕ, $\partial\phi/\partial n$) at time t. Second-order coefficients are expressed as D/Dt of Eqs. (2) and (3), and are calculated using the solution of a second BIE for ($\partial\phi/\partial t$, $\partial^2\phi/\partial t\partial n$), for which boundary conditions are obtained from the solution of the first BIE and the time derivative of boundary conditions of the first BIE problem. Detailed expressions for the Taylor series can be found in Grilli and Subramanya (1996).

VOF model

Guignard *et al.* (2001) developed a numerical model for simulating multi-interface two-phases (air/water) viscous incompressible flows (Fig. 2). This model uses a Volume of Fluid Method for the interface representation, together with a solution of Navier-Stokes (NS) equations in both fluids, with respect to their actual density. In the NS solver, an additional equation is introduced, according to the pseudo-comppressibility method (De Jouëtte et al., 1991), which uses a pseudo-time variable, over which NS equations are solved, using a 5th-order Runge-Kutta scheme (see Biausser et al., 2003a, for detail). An orthogonal grid with variable mesh, covering both fluids, is defined along the x and z directions and NS equations are solved at the center of each grid cell (finite volume spatial scheme).

Interfaces and their motion are time-updated using a new Lagrangian method referred to as SL-VOF method (with SL indicating the piecewise linear segments that are used to represent interfaces). In this method, interfaces are modeled two ways : (i) a *color* function is defined within each cell of the VOF grid, as the fraction (0 to 1) of the cell area filled with the denser fluid (classical VOF concept); hence, any fraction less than one and more than zero indicates the presence of an interface in this cell; (ii) a multi-segmental representation of the interfaces is defined based on the values of the color function, according to a so-called "Piecewise Linear Interface Calculation" concept. This latter method is second-order in volume conservation. Interface segments are advected, as a function of time, based on Lagrangian markers, following the velocity field obtained from the solution of NS equations (first-order method). After this advection, new values of the color function are computed, which take into account the new position of the interface segments.

Principle of model coupling

In the coupling algorithm, each model has to provide the other one with initial and boundary conditions, consistent with the physical problem treated.

For the *weak coupling method*, computations in the BEM and VOF models are somewhat de-coupled in the sense that the VOF model is initialized with BEM results only once. The VOF model is then provided with offshore boundary conditions on a lateral matching boundary, which are pre-calculated as a function of time in the BEM model. These boundary conditions only have to be interpolated in both (vertical) space and time based on the VOF grid cell height and time step size. In some cases, when the matching boundary is far enough offhore, a no-flow condition can even be assumed (this will be the case in the present applications of the weak coupling method), which fully uncouples the BEM and VOF models, beyond the single initialization of VOF computations.

In the *strong coupling method*, both BEM and VOF models overlap in a spatial region (Fig. 3) and computations are fully coupled, with both models constantly exchanging information in realtime. More specifically, say, at step t^n, the VOF model requires values of velocity and pressure at its leftward vertical boundary. These are calculated based on values of the potential, and its temporal and spatial derivatives, on the entire boundary of the BEM domain. At the same time-step, the BEM model requires values of $\partial\phi/\partial n$ and $\partial^2\phi/\partial n\partial t$ at its rightward boundary. These are deduced from known values of horizontal velocity components,u^n, calculated in the VOF model as, $\partial\phi/\partial n = u^n$, and $\partial^2\phi/\partial n\partial t = (u^n - u^{n-1})/\Delta t^n$.

The exchange of boundary conditions between models is made through using common data files while running both models simultaneously (ideally on two different processors, as

parallelization reduces computing time).

APPLICATIONS

Validation with experiments

As a first example of results of model coupling, the shoaling and breaking of a solitary wave of initial height $H_o/h_o = 0.45$ is calculated over a 1:15 slope. This case, which leads to a large scale plunging breaker, was modeled by Grilli *et al.* (1997) with the BEM model, up to impending jet impact (Fig. 1). Li and Raichlen (1998) compared these FNPF computations to detailed laboratory experiments and showed a good agreement for wave shapes, up to the stage of curve f in Fig. 1.

Figs. 2 and 3 show results of the BEM-VOF model for this case, for weak and strong coupling, respectively; in the second case, the VOF grid had 825 by 80 cells in the x and y directions, respectively. The breaker jet impact occurs in very shallow water, which leads to air trapping and to a rebound creating a new, forward moving, jet. Such features are well observed in laboratory experiments.

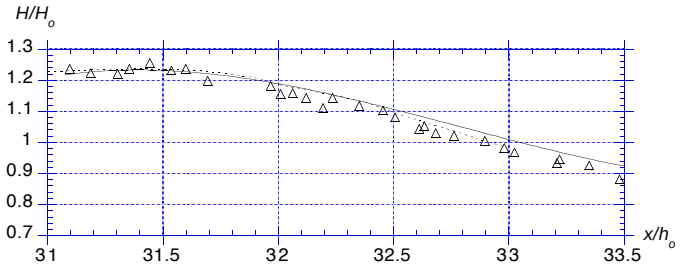

Fig. 4 : Cases of Figs. 1,2,3. (- - - - -) BEM results (Grilli *et al.*, 1997); (——) strongly coupled FNPF-BEM/NS-VOF results; (△) Li and Raichlen's (1998) experiments.

Fig. 4 shows a comparison of the change in wave height H/H_o, calculated as a function of x/h_o in both the BEM and the strongly coupled BEM-VOF models, with Li and Raichlen's experiments. Both models agree well with each other, and with the experiments, up to the stage of curve f in Fig. 1 ($x/h_o = 32.7$). Beyond that, the BEM-FNPF model quickly fails; but the agreement of the VOF-BEM model with experiments can still be considered as quite good (considering the experimental variance). This indicates that the VOF method is accurate for modeling such post-breaking waves.

Note that, in these computations, the molecular value of the kinematic viscosity was used in the NS solver. This implies that, for the grid cell size used, viscous forces are quite small compared to inertia forces and, hence, are negligible. This also means that Euler equations rather than NS equations are solved in the model, and viscous dissipation at sub-grid scales is not correctly represented in the results. To do so, a turbulence closure scheme should be used and/or even smaller grid cells. Although several standard turbulence schemes have been implemented in the NS solver, we elected not to use them at this stage and leave this for further studies. It should also be pointed out that some amount of numerical dissipation always exists in the model, which should be correctly assessed before a turbulence scheme is calibrated for breaking waves. Looking at Fig. 4, however, the good agreement of the computed reduction in wave height with laboratory measurements indicates that, for this case, no significant dissipation at subgrid scales has yet occurred, at least beyond the numerical dissipation inherent to the NS solver.

Effect of slope on breaking type

The weak BEM-VOF coupling modeling methodology is now used to compute various cases of solitary wave breaking over various slopes, between 1:8 and 1:100. All of the following results correspond to a wave with initial height $H_o/h_o = 0.5$ in an offshore constant depth region. The VOF domain is made of two finely discretized subdomains of 580x200 and 340x200 cells, in the horizontal and vertical directions, respectively. In each computations, there are typically hundreds of time steps (e.g., 700 for the 1:8 slope for a total physical time of 2.19 s), and there are 40 pseudo-time steps for each actual time step. Full results are saved every 10 time steps. Computations were performed on a two-processor 666 MHz DEC ALPHA workstation, and computations were run in parallel for each subdomain on the two processors, with a CPU time of 3.73 s per pseudo-time step (this, e.g., leads to a total computational time of 29 h for the 1:8 slope case below).

We first look at detailed results for a wave breaking on a 1:15 slope. Fig. 5 shows the development, impact, and rebound of a large plunging breaker, with an enclosed air pipe. On this steep slope, the wave height does not increase very much beyond its intial value, and the wave becomes unstable when its height is about twice the local depth. In Figs. 5a,b, and c, we see very large water velocities occur in both the plunging and the rebound jets. Note that only a small number of velocity vectors are plotted to make the figures readable. Hence, it is difficult to assess the strength of the recirculation that occurs below the jet, after breaking. Other computations performed with a three-dimensional VOF model by Biausser et al. (2003b), for a similar 2D breaking case, show that vorticity is almost non-existent during wave overturning, before the jet impacts on the forward water surface, except at the apex of the internal air cavity enclosed below the jet and along the bottom and free surface boundaries (these regions cannot be seen on the figures because of a lack of resolution due to the small number of velocity vectors that are shown). This near absence of vorticity in the bulk of the fluid flow confirms the relevance of inviscid, and even irrotationnal, flow computations prior to the occurrence of wave breakin, as done in FNPF-BEM models.

Computations can be pursued beyond the stage of Fig. 5c but, as indicated in an above section, viscous dissipation, which is not accurately calibrated in the model, will become increasingly more important at these later stages of breaking. Fig. 5d, for instance, shows some of these computed later stages and how the main wave first collapses on the slope, followed by the rebound jet, which also crashes on and runs up the slope.

Fig. 6 shows the propagation and breaking of a wave of identical characteristics, over a much steeper 1:8 slope. Here, we see the formation of a surging breaker, whose lower part becomes unsta-

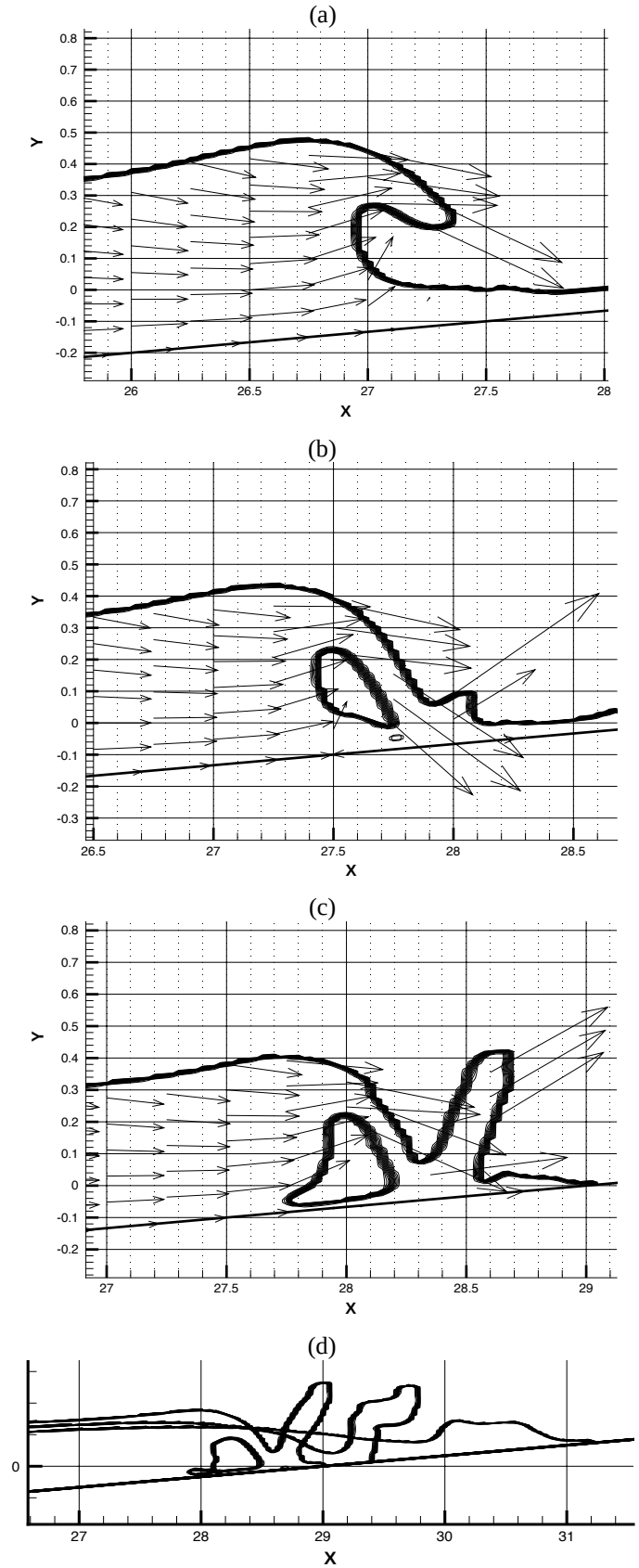

Fig. 5 : Weak FNPF-BEM/NS-VOF coupling computation of a solitary wave of height $H_o/h_o = 0.5$ breaking over a 1:15 slope: Three stages of plunging breaking (a)-(c); three stages of breaker collapsing (d).

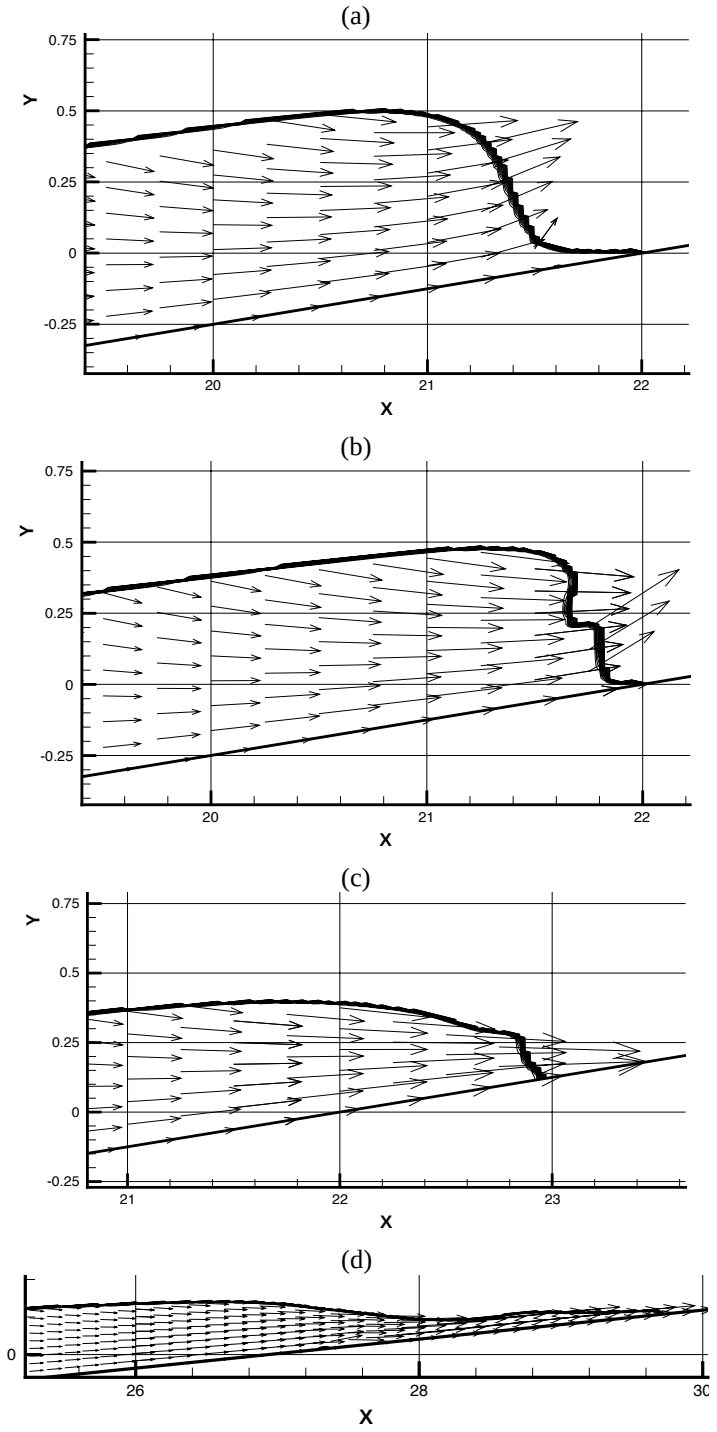

Fig. 6 : Weak FNPF-BEM/NS-VOF coupling computation of a solitary wave of height $H_o/h_o = 0.5$ breaking over a 1:8 slope: Four stages of surging breaking.

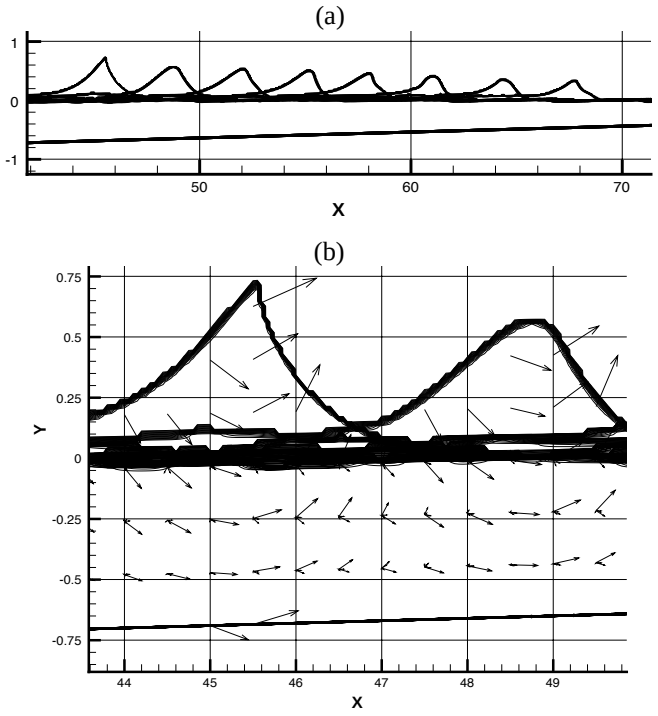

Fig. 7 : Weak FNPF-BEM/NS-VOF coupling computation of a solitary wave of height $H_o/h_o = 0.5$ breaking over a 1:100 slope: Stages of spilling breaking.

ble and shoots up the slope as a jet of reducing thickness. Viscous dissipation is mainly limited to bottom friction and we see a significant wave runup. At breaking, the wave height is still about equal to its incident value. However, this also corresponds to about five times the local depth. Looking at velocity vectors in Figs. 6a,b, abd c, we see velocities are very uniform over depth and the whole wave first moves up the slope as a bore. After breaking, however, we see in Fig. 6d some much larger velocities occurring in the thin water jet at the top of the slope.

Finally, Fig. 7 shows the propagation and spilling breaking of the same wave on a very mild 1:100 slope. As expected for this type of breaking, the wave height significantly increases,due to both stronger and longer nonlinear wave-slope interactions, by about 50%, as compared to the initial value, and exhibits a small size instability at the crest, i.e., the roller, when it reaches a height on the order of the local depth.

CONCLUSIONS

We implemented and validated a model based on couplig a BEM model solving FNPF equations and a VOF model solving NS equations. We derived and tested two coupling methodologies, referred to as *weak and strong* coupling. We compared results of the strongly coupled model to laboratory experiments and showed the agreemeent for wave height beyond breaking was quite good. For more efficiency, we applied the weakly coupled model to the shoaling and breaking of solitary waves on slopes. By varying the slope, we obtained plunging, surging, and spilling breaker types. Computations were pursued with the VOF model into post-breaking stages without any difficulties.

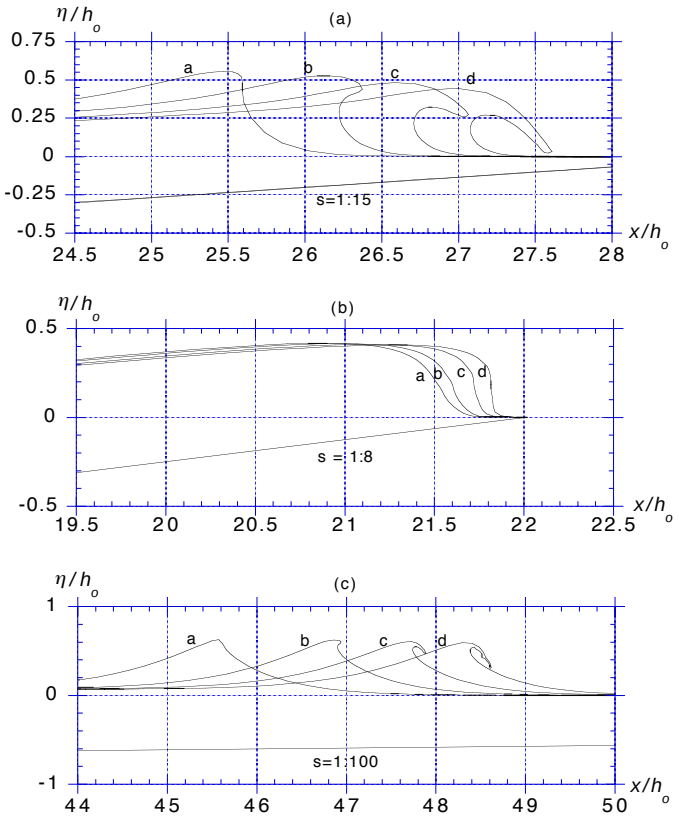

Fig. 8 : BEM computations of a solitary wave of height $H_o/h_o = 0.45$ breaking over a : (a) 1:15; (b) 1:8; and (c) 1:100 slope. Adapted from Grilli et al. (1997).

Grilli et al. (1997) computed cases similar to those in Figs. 5 to 7, using their BEM model. Their computed waves at and slightly beyond breaking are reproduced in Fig. 8, for a solitary wave with initial height $H_o/h_o = 0.45$, i.e., slightly smaller than used here with the BEM/VOF model. BEM computations broke down slightly beyond the stage of curves d in each case in Fig. 8, i.e., at jet impact in the first and third cases (Figs. 8a,c), and during runup in the second case (Fig. 8b). At breaking, we see a strong similarity of BEM and BEM/VOF results. In the first and third cases, BEM and BEM/VOF wave heights are in close agreement, despite the use of a smaller wave in BEM computations. This is due to numerical dissipations in the VOF model, which are significant for longer distances of propagation over mild slopes. In the second case, with a steeper slope, the VOF model does not cause yet significant dissipation and reduction of wave height. Hence, BEM wave heights are smaller than BEM/VOF wave heights at breaking, in accordance with the magnitude of the incident wave used.

The present BEM/VOF computations are thus deemed to be accurate to propagate the wave until breaking, while they do not have the limitations of the former BEM computations to prior to jet impact (e.g., Fig. 8u). The present model thus allows to compute characteristics of breaking and post-breaking waves on slopes, including maximum runup. For the latter value, as pointed out

before, a more carefull assessment and calibration of turbulent dissipation in the model should be made.

More cases will be shown and discussed in detail during the conference.

ACKNOWLEDGEMENTS

The authors wish to acknowledge support from the French National Program PATOM (Programme Atmosphère et Océan à Multi-échelles).

The third author wishes to acknowledge support for this research from the Office of Naval Research, under grant No. N-00014-01-10349 of the US Department of the Navy, Office of the Chief of Naval Research, and from the US National Science Foundation, under grant No. CMS-0100223.

REFERENCES

Biausser, B., Grilli, S.T., and Fraunié (2003a). "Numerical simulations of three-dimensional wave breaking by coupling of a VOF method and a Boundary Element method," *Proc. 13th Offshore and Polar Engng. Conf.* (ISOPE03, Honolulu, HI, May 2003) (to appear).

Biausser, B., Grilli, S.T., and Fraunié (2003b). "Numerical analysis of the internal kinematics and dynamics of three-dimensional breaking waves on slopes," *Proc. 13th Offshore and Polar Engng. Conf.* (ISOPE03, Honolulu, HI, May 2003) (to appear).

De Jouëtte, C., Viviand, H., Wornom, S. and Le Gouez, J.M. (1991). "Pseudo-Compressibility Methods for Incompressible Flow Calculation," *Proc 4th International Symposium on Computational Fluid Dynamics*, University of California, Davis.

Grilli, S.T. and J. Horrillo (1997). "Numerical generation and absorption of fully nonlinear periodic waves," *J. Engng. Mech.*, Vol 123(10), pp 1060-1069.

Grilli, S.T. and Horrillo, J. (1999) "Shoaling of periodic waves over barred-beaches in a fully nonlinear numerical wave tank," *J. Offshore and Polar Engng.*,**9**(4), 257-263.

Grilli, S.T., Svendsen, I.A. and R., Subramanya (1997) "Breaking criterion and characteristics for solitary waves on slopes," *J. Waterway Port Coastal and Ocean Engng.,* Vol 123(3), pp 102-112.

Grilli, S.T. and R., Subramanya (1996) "Numerical modeling of wave breaking induced by fixed or moving boundaries," *Computational Mech.*, Vol 17, pp 374-391.

Grilli, S.T., Subramanya, R., Svendsen, I.A. and J., Veeramony (1994) "Shoaling of solitary waves on plane beaches," *J. Waterway Port Coastal and Ocean Engng.,* Vol 120(6), pp 609-628.

Grilli, S.T., Svendsen, I.A., and Subramanya, R. (1997) Breaking Criterion and Characteristics for Solitary Waves on Slopes. *J. Waterways Port Coastal Ocean Engng.,* **123**(3), 102-112.

Guignard, S., Grilli, S.T., Marcer, R. and Rey, V. (1999) "Computation of shoaling and breaking waves in nearshore areas by the coupling of BEM and VOF methods," *Proc. 9th Offshore and Polar Engng. Conf.* (ISOPE99, Brest, France, May 1999), Vol. III, 304-309.

Guignard, S., Marcer, R., Rey, V., Kharif, Ch., and Ph. Fraunié (2001) "Solitary Wave Breaking on Sloping Beaches : 2D two-phase Flow Numerical Simulation by SL-VOF Method," *Eur. J. Mech. B-Fluids,* **20**, 57-74.

Kim, C.H., Clément, A.H. and K., Tanizawa (1999) "Recent Research and Development of Numerical Wave Tank—A review," *Intl. J. Offshore and Polar Engng.*, **9**(4), 241-256.

Li, Y. and F. Raichlen (1998) "Breaking criterion and characteristics for solitary waves on slopes — Discussion," *J. Waterways Port Coastal Ocean Engng.*, **124**(6), 329-333.

Ohyama, T., Beji, S., Nadaoka, K., and Battjes, J.A. (1994) "Experimental verification of numerical model for nonlinear wave evolution," *J. Waterway Port Coastal and Ocean Engng.*, **120**(6), 637-644.